Electronic Supplementary Material (ESI) for Journal of Materials Chemistry A.

C_3 Production from CO_2 Reduction by Concerted *CO Trimerization on Single-Atom Alloy Catalyst

Ling Chen[a], Cheng Tang[a], Yao Zheng[a], Egill Skúlason[b] and Yan Jiao[a]*

[a] School of Chemical Engineering and Advanced Materials, The University of Adelaide, SA 5005, Australia

[b] Science Institute and Faculty of Industrial Engineering, Mechanical Engineering and Computer Science, University of Iceland, Reykjavík, Iceland

Corresponding author: *yan.jiao@adelaide.edu.au

This file includes:

- **Table S1-S6**
- **Figure S1-S24**
- **Supplymentary Note 1**
- **Supplementary Reference**

Table S1. Energy for gas phase species. Units are in eV.

Gas Molecule	E (eV)	ZPE (eV)	–TS (eV)	G (eV)
H_2 (g)	–6.75	0.27	–0.41	–6.89
H_2O (g)	–14.22	0.56	–0.67	–14.33
CO (g)	–14.78	0.13	–0.61	-15.26
CO_2 (g)	–23.01	0.31	–0.66	–23.36
CH_4 (g)	–24.01	1.19	–0.57	–23.39
C_2H_4 (g)	–31.97	1.37	–0.55	–31.15
C_2H_5OH (g)	–46.88	2.13	–0.60	–45.35
$C_3H_6(OH)_2$ (g)	–69.99	3.64	–0.68	–67.03

Table S2. *CO binding energies from various adsorption sites on Cu-DAN.[1]

***CO adsorption sites**		**E_{*CO} /eV (PBE)**	**E_{*CO} /eV (RPBE)**	**difference**
Atop @ basal plane	(111) facet top	–0.75	–0.55	–0.20
	(100) facet top	–0.73	-0.52	-0.21
Bridge @ basal plane	(111) facet bridge	–0.80	-0.49	-0.29
	(100) facet bridge	–0.77	-0.50	-0.27
Hollow @ basal plane	(111) 3-fold fcc	–0.91	-0.65	-0.26
	(111) 3-fold hcp	–0.80	-0.58	-0.22
	(100) 4-fold	–0.90	-0.66	-0.24
Bridge @ edge	(100)/(111) boundary bridge	–1.06	-0.78	-0.28
	(100)/(100) boundary bridge	–0.92	-0.69	-0.23
	(111)/(111) boundary bridge	atom moved to boundary top		
Atop @ edge	(111)/(111) boundary top	–0.99	-0.81	-0.18
	(100)/(111) boundary top	–1.02	-0.83	-0.19
	(100)/(100) boundary top	–1.13	-0.95	-0.18
	(100)/(100) boundary top 2	–1.04	-0.87	-0.17
Average				-0.22

Table S3. Free energy of 3*CO adsorption (ΔG_{3*CO}) and formation free energy for $\Delta G_{*CO-CO-COH}$ on 17 sites of pristine Cu-DAN and Ag@Cu-DAN. The results are presented in three groups based on individual *CO adsorption strength. The energy unit is eV.

Group	Site	Structure	ΔG_{3*CO}	$\Delta G_{*CO-CO-COH}$
1 (2 strong + 1 weak *CO)	1	Cu-DAN	–1.74	1.79
		Ag @ Cu-DAN	–1.48	1.23
	2	Cu-DAN	–1.64	1.59
		Ag @ Cu-DAN	–1.40	1.14
	3	Cu-DAN	–1.54	1.36
		Ag @ Cu-DAN	–1.46	1.06
	4	Cu-DAN[a]	–1.62	1.25
2 (1 strong + 2 weak *CO)	5	Cu-DAN[a]	–1.55	1.11
	6	Cu-DAN	–1.33	1.05
		Ag @ Cu-DAN	–1.22	0.67
	7	Cu-DAN[a]	–1.42	1.03
	8	Cu-DAN[a]	–1.46	0.99
	9	Cu-DAN	–1.33	0.93
		Ag @ Cu-DAN	–1.20	0.75
	10	Cu-DAN[a]	–1.38	0.91
	11	Cu-DAN[a]	–1.25	0.90
	12	Cu-DAN	–1.26	0.79
		Ag @ Cu-DAN	–1.06	0.60
	13	Cu-DAN[a]	–1.02	0.74
3 (3 weak *CO)	14	Cu-DAN[a]	–0.91	0.80
	15	Cu-DAN	–1.18	0.62
		Ag @ Cu-DAN	–1.1	0.45
	16	Cu-DAN[a]	–0.87	0.92
	17	Cu-DAN[a]	–0.93	0.95

[a] ΔG_{3*CO} and ΔG are not calculated on Ag@ Cu-DAN structures, due to that the adsorption centre being not close to the Ag doping, therefore assuming the adsorption behaviour will not be affected.

Table S4. Reaction energy for different reaction steps (ΔE) and the corresponding activation barrier (E_a) on site 10, 11, and 15 of pristine Cu-DAN. Corresponding MEP could be found in Figures S19 – S21.

Site	Reaction Steps	Δ*E*	E_a
10	*CO+*CO+*CO→*CO–CO–CO	1.05	1.33
11	*CO+*CO+*CO→*CO–CO–CO	0.77	1.23
15	*CO+*CO+*CO→*CO–CO–CO	-0.01	0.67
	*CO + *H^-→*CHO	0.82	0.89
	*CO + *CO + *H^-→*CO–COH	0.73	1.18

Table S5. Thermodynamic profile regarding all PCET steps after *CO trimerization. The energy unit is eV. The favourable species are colored in black while less favorable species are displayed in red.

PCET step	Reaction Step	ΔG
7th	*CO+*CO+*CO →*CO–CO–CO	–0.01
	* CO–CO–CO + H^++e^-→*CO–CO–COH	0.46
8th	*CO–CO–COH+H^++e^-→*COH–CO–COH	–0.06
	*CO–CO–COH+H^++e^-→*CO–CHO–COH	0.95
9th	*COH–CO–COH+H^++e^-→*CHOH–CO–COH	–0.12
	*COH–CO–COH+H^++e^-→*C–CO–COH + H_2O	1.20
10th	*CHOH–CO–COH+H^++e^-→*CHOH–CO–CHOH	–0.44
	*CHOH–CO–COH+H^++e^-→*CHOH–CO–C + H_2O	–0.24
	*CHOH–CO–COH+H^++e^-→*CH–CO–COH + H_2O	–0.10
11th	*CHOH–CO–CHOH+H^++e^-→*CH_2OH–CO–CHOH	–0.40
	*CHOH–CO–CHOH+H^++e^-→*CH–CO–CHOH + H_2O	–0.02
12th	*CH_2OH–CO–CHOH+H^++e^-→*CH_2OH–CO–CH_2OH	–0.01
	*CH_2OH–CO–CHOH+H^++e^-→*CHOH–CO–CH_2 + H_2O	0.63
	*CH_2OH–CO–CHOH+H^++e^-→*CH–CO–CH_2OH + H_2O	1.58
13th	*CH_2OH–CO–CH_2OH+H^++e^-→*CH_2OH–CHO–CH_2OH	–0.41
	CH_2OH–CO–CH_2OH+H^++e^-→CH_2OH–CHO–CH_2 + H_2O	–0.32
14th	*CH_2OH–CHO–CH_2OH+H^++e^-→*CH_2OH–CHOH–CH_2OH	0.06
	CH_2OH–CHO–CH_2OH+H^++e^-→CH_2OH–CH_2–CH_2OH + *O	0.23
15th	*CH_2OH–CHOH–CH_2OH+H^++e^-→*CH_2OH–CHOH–CH_2 + H_2O	0.19
	CH_2OH–CHOH–CH_2OH+H^++e^-→CH_2OH–CH(OH_2)–CH_2OH + H_2O	0.55
16th	*CH_2OH–CHOH–CH_2+H^++e^-→ *CH_2OH–CHOH–CH_3	–0.79
	*CH_2OH–CHOH–CH_3→ CH_2OH–CHOH–$CH_{3(g)}$	0.38

Table S6: The free energy contributions of the key reaction intermediates along the 1,2-propanediol pathway. The energy unit is eV.

Intermediates	E	ZPE	–TS	G
*CO–CO–CO	–334.13	0.51	–0.30	–333.92
*CO–CO–COH	–337.50	0.95	–0.32	–336.87
*COH–CO–COH	–341.29	1.27	–0.34	–340.36
*CHOH–CO–COH	–345.06	1.54	–0.36	–343.88
*CHOH–CO–CHOH	–349.15	1.91	–0.48	–347.72
*CH_2OH–CO–CHOH	–353.25	2.22	–0.51	–351.54
*CH_2OH–CO–CH_2OH	–356.86	2.48	–0.59	–354.97
*CH_2OH–CHO–CH_2OH	–361.08	2.83	–0.53	–358.78
*CH_2OH–CHOH–CH_2OH	–364.55	3.08	–0.67	–362.14
*CH_2OH–CHOH–CH_2 + H_2O(g)	–368.07	3.28	–0.58	–365.37
*CH_2OH–CHOH–CH_3 + H_2O(g)	–372.58	3.67	–0.66	–369.57
$C_3H_6(OH)_2$ (g) + H_2O(g)	–372.16	3.64	–0.68	–369.19

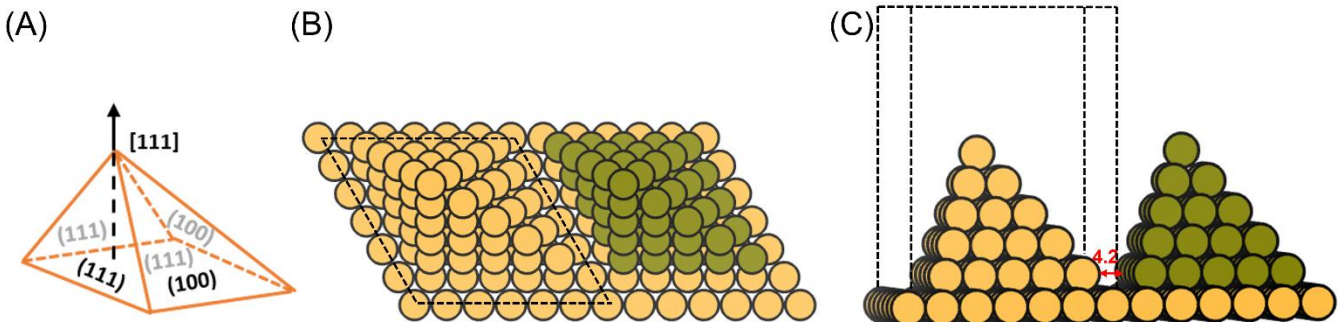

Figure S1. (A) Schematic illustration of [111] Cu diamond nanopyramid[1]. (B) Top and (C) side view on the atomic structure of the densely arrayed Cu nanopyramid, which is constructed based on a 6×6×1 Cu (111) surface with 4.2 Å pitch from adjacent Cu nanopyramids to represent the dense-array. Solid blue lines serve as visual guides to show the Cu atoms on the edge. Black dashed lines depict the unit cell. Colour codes: Cu, orange and green.

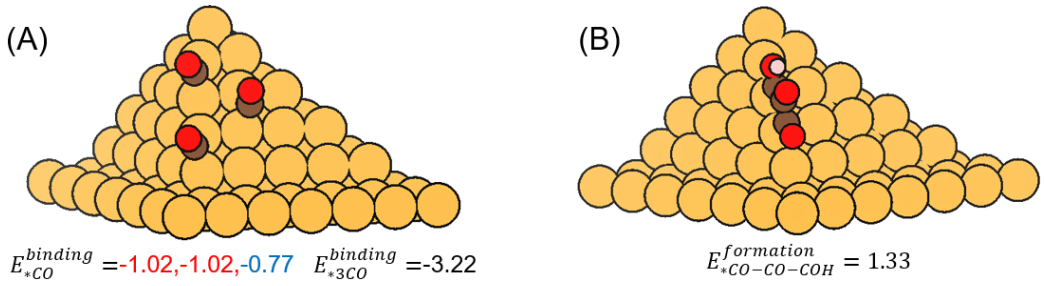

Figure S2. Atomic structures of adsorption of (A) three *CO and (B) *CO–CO–COH on reaction Site 1 from **Group 1** and the relevant adsorption energies (eV). Colour codes: Cu, orange; C, brown; O, red and H, pink. Red and blue values denote strong and weak *CO adsorption energies,[1] respectively.

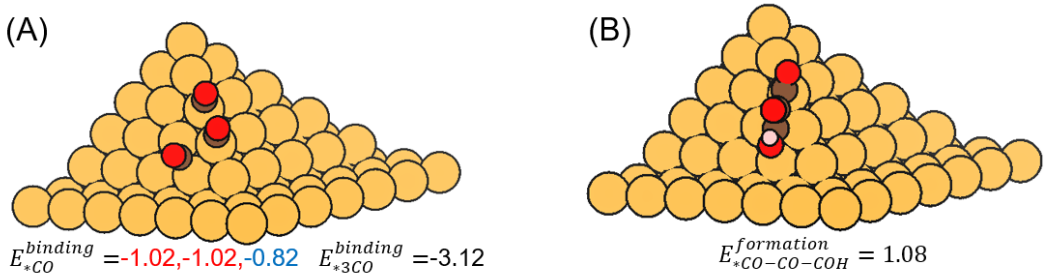

Figure S3. Atomic structures of adsorption of (A) three *CO and (B) *CO–CO–COH on reaction Site 2 from **Group 1** and the relevant adsorption energies (eV). Colour codes: Cu, orange; C, brown; O, red and H, pink. Red and blue values denote strong and weak *CO adsorption energies, respectively.

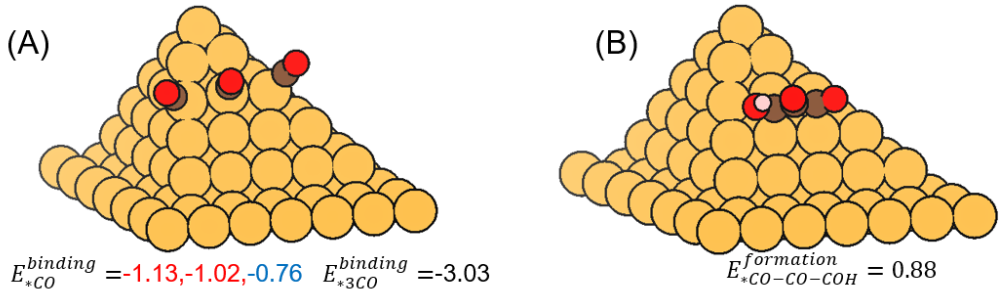

Figure S4. Atomic structures of adsorption of (A) three *CO and (B) *CO–CO–COH on reaction Site 3 from **Group 1** and the relevant adsorption energies (eV). Colour codes: Cu, orange; C, brown; O, red and H, pink. Red and blue values denote strong and weak *CO adsorption energies, respectively.

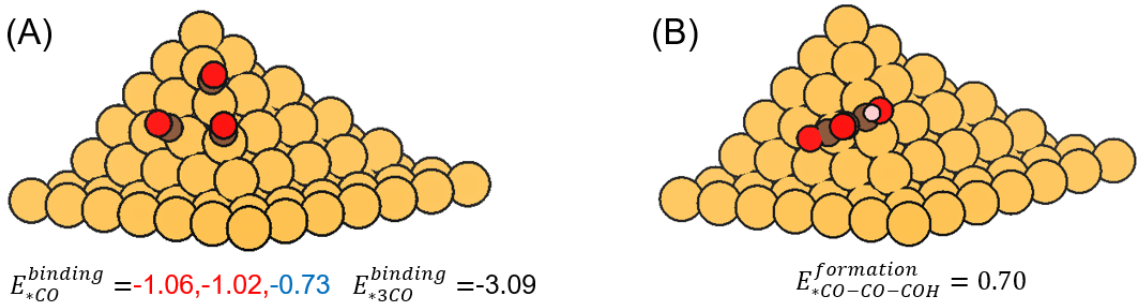

Figure S5. Atomic structures of adsorption of (A) three *CO and (B) *CO–CO–COH on reaction Site 4 from **Group 1** and the relevant adsorption energies (eV). Colour codes: Cu, orange; C, brown; O, red and H, pink. Red and blue values denote strong and weak *CO adsorption energies, respectively.

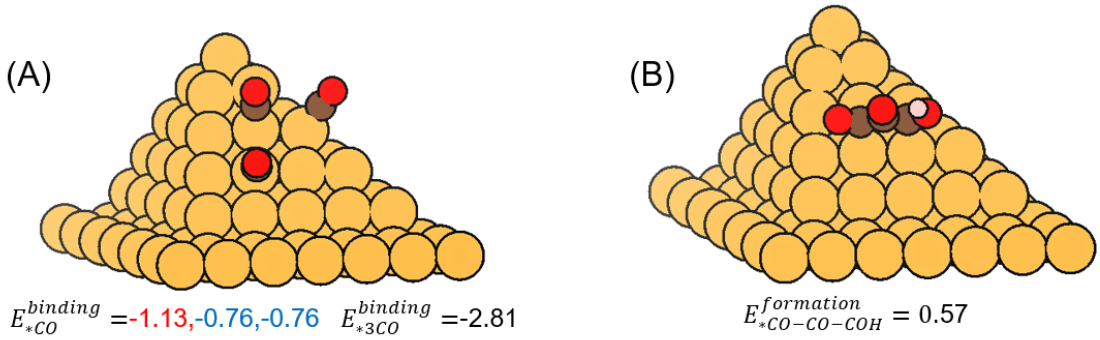

Figure S6. Atomic structures of adsorption of (A) three *CO and (B) *CO–CO–COH on reaction Site 5 from **Group 2** and the relevant adsorption energies (eV). Colour codes: Cu, orange; C, brown; O, red and H, pink. Red and blue values denote strong and weak *CO adsorption energies, respectively.

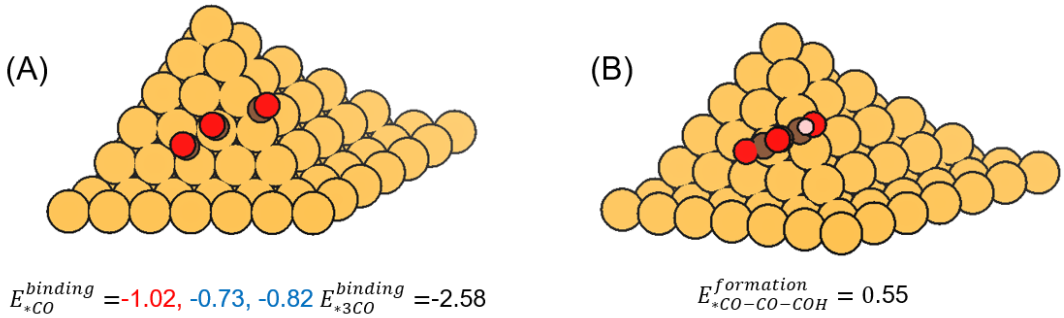

Figure S7. Atomic structures of adsorption of (A) three *CO and (B) *CO–CO–COH on reaction Site 6 from **Group 2** and the relevant adsorption energies (eV). Colour codes: Cu, orange; C, brown; O, red and H, pink. Red and blue values denote strong and weak *CO adsorption energies, respectively.

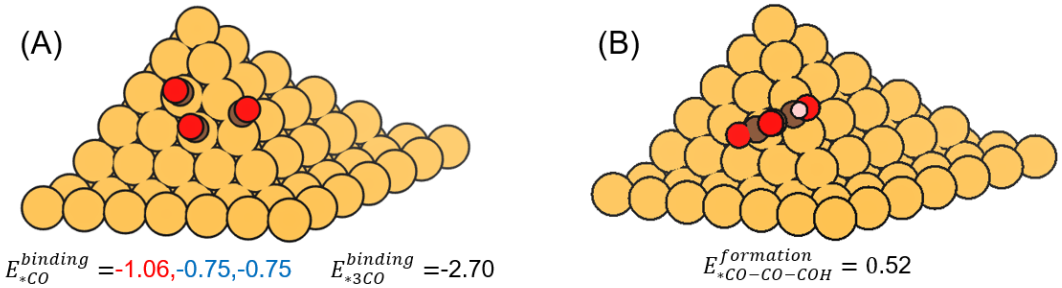

Figure S8. Atomic structures of adsorption of (A) three *CO and (B) *CO–CO–COH on reaction Site 7 from **Group 2** and the relevant adsorption energies (eV). Colour codes: Cu, orange; C, brown; O, red and H, pink. Red and blue values denote strong and weak *CO adsorption energies, respectively.

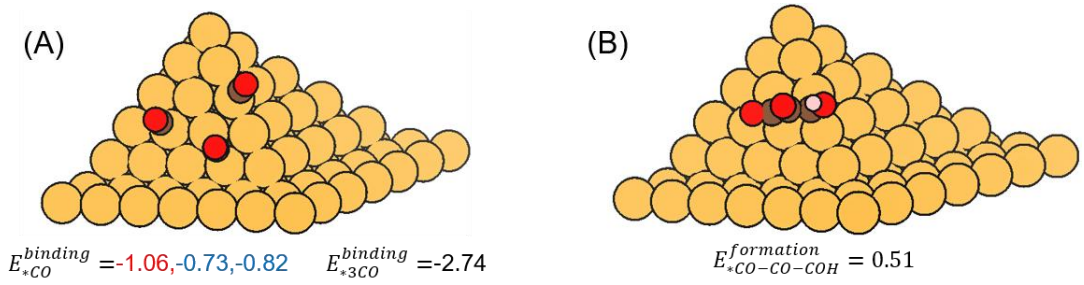

Figure S9. Atomic structures of adsorption of (A) three *CO and (B) *CO–CO–COH on reaction Site 8 from **Group 2** and the relevant adsorption energies (eV). Colour codes: Cu, orange; C, brown; O, red and H, pink. Red and blue values denote strong and weak *CO adsorption energies, respectively.

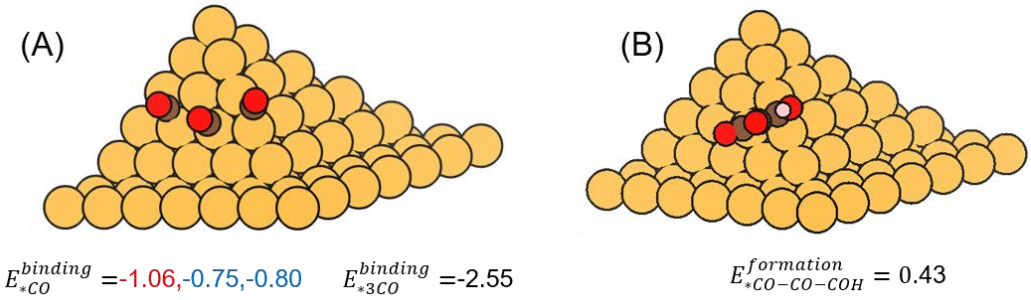

Figure S10. Atomic structures of adsorption of (A) three *CO and (B) *CO–CO–COH on reaction Site 9 from **Group 2** and the relevant adsorption energies (eV). Colour codes: Cu, orange; C, brown; O, red and H, pink. Red and blue values denote strong and weak *CO adsorption energies, respectively.

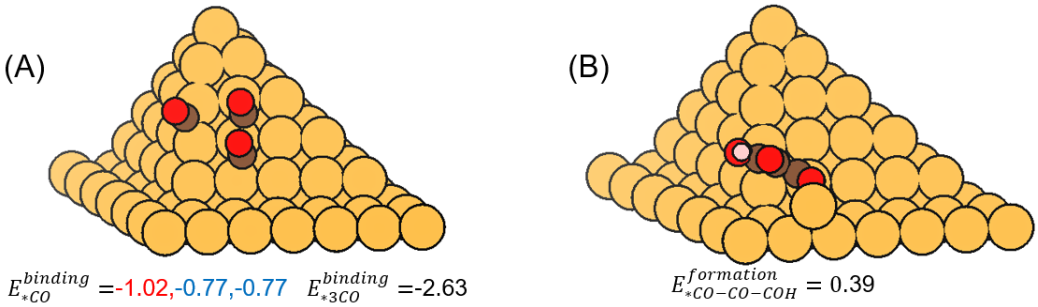

Figure S11. Atomic structures of adsorption of (A) three *CO and (B) *CO–CO–COH on reaction Site 10 from **Group 2** and the relevant adsorption energies (eV). Colour codes: Cu, orange; C, brown; O, red and H, pink. Red and blue values denote strong and weak *CO adsorption energies, respectively.

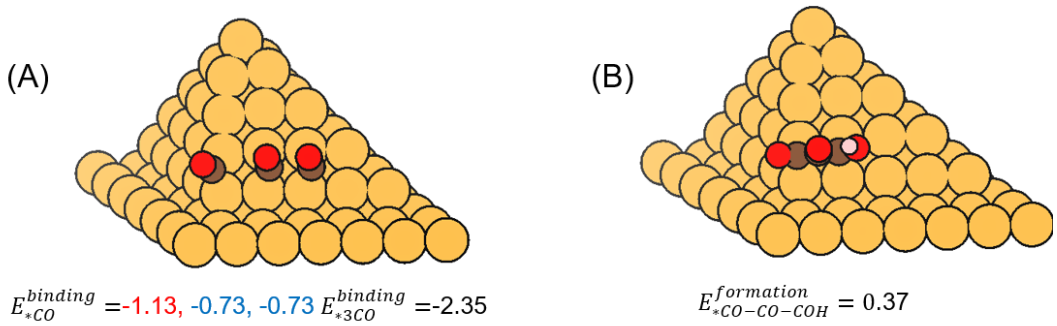

Figure S12. Atomic structures of adsorption of (A) three *CO and (B) *CO–CO–COH on reaction Site 11 from **Group 2** and the relevant adsorption energies (eV). Colour codes: Cu, orange; C, brown; O, red and H, pink. Red and blue values denote strong and weak *CO adsorption energies, respectively.

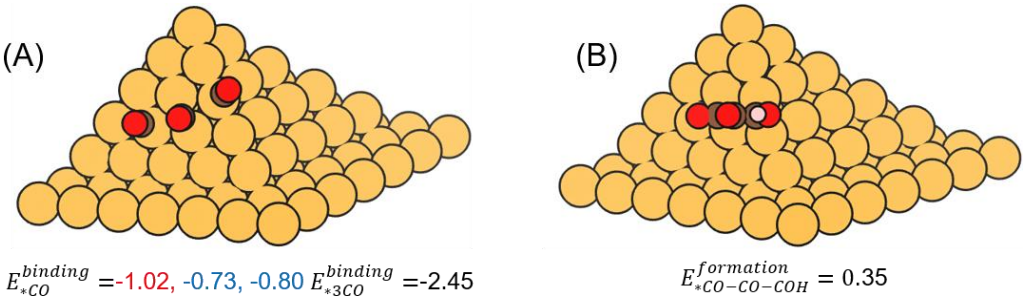

Figure S13. Atomic structures of adsorption of (A) three *CO and (B) *CO–CO–COH on reaction Site 12 from **Group 2** and the relevant adsorption energies (eV). Colour codes: Cu, orange; C, brown; O, red and H, pink. Red and blue values denote strong and weak *CO adsorption energies, respectively.

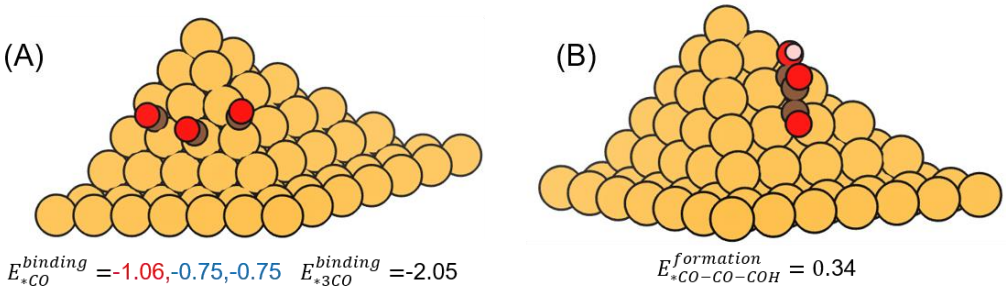

Figure S14. Atomic structures of adsorption of (A) three *CO and (B) *CO–CO–COH on reaction Site 13 from **Group 2** and the relevant adsorption energies (eV). Colour codes: Cu, orange; C, brown; O, red and H, pink. Red and blue values denote strong and weak *CO adsorption energies, respectively.

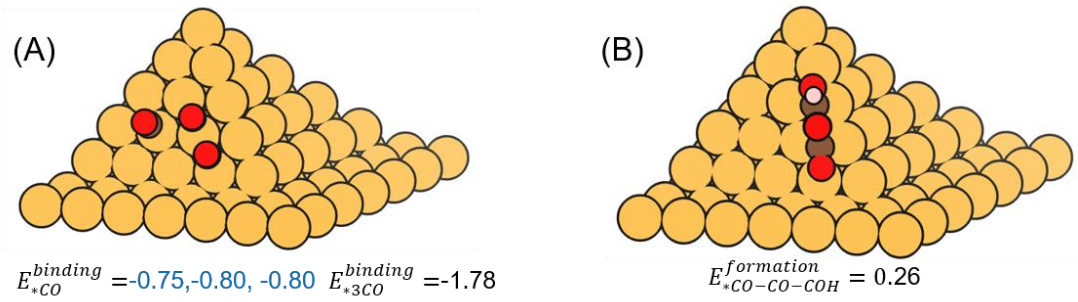

Figure S15. Atomic structures of adsorption of (A) three *CO and (B) *CO–CO–COH on reaction Site 14 from **Group 3** and the relevant adsorption energies (eV). Colour codes: Cu, orange; C, brown; O, red and H, pink. Red and blue values denote strong and weak *CO adsorption energies, respectively.

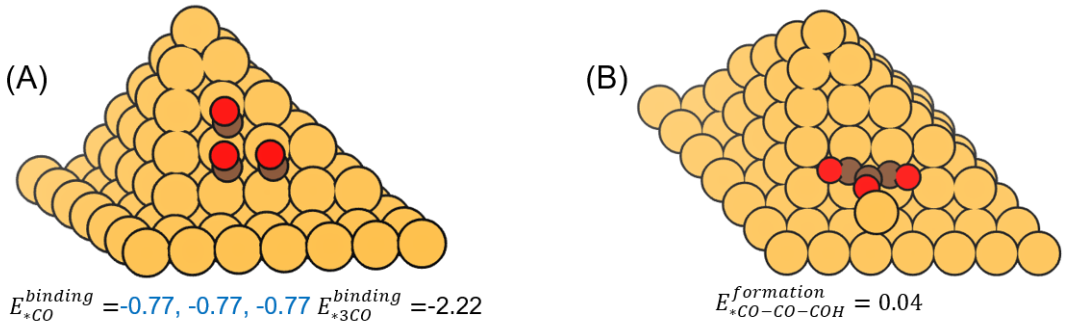

Figure S16. Atomic structures of adsorption of (A) three *CO and (B) *CO–CO–COH on reaction Site 15 from **Group 3** and the relevant adsorption energies (eV). Colour codes: Cu, orange; C, brown; O, red and H, pink. Red and blue values denote strong and weak *CO adsorption energies, respectively.

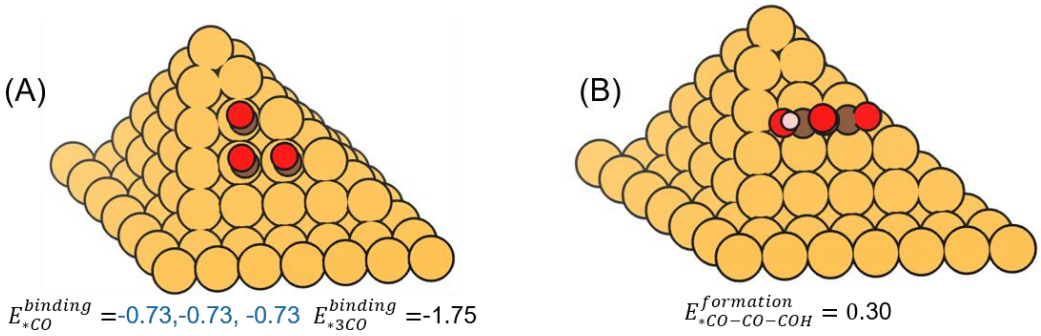

Figure S17. Atomic structures of adsorption of (A) three *CO and (B) *CO–CO–COH on reaction Site 16 from **Group 3** and the relevant adsorption energies (eV). Colour codes: Cu, orange; C, brown; O, red and H, pink. Red and blue values denote strong and weak *CO adsorption energies, respectively.

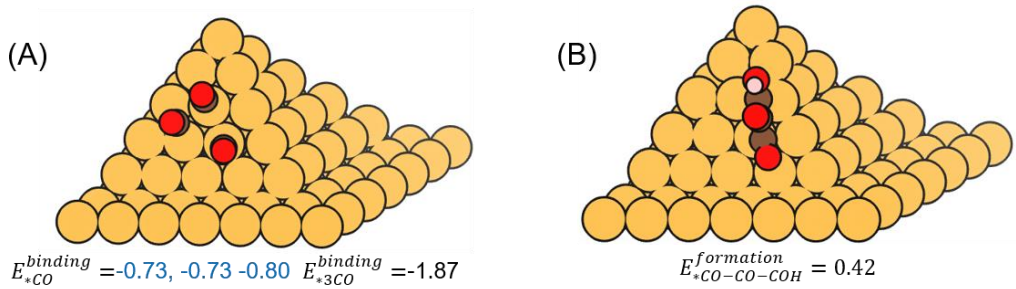

Figure S18. Atomic structures of adsorption of (A) three *CO and (B) *CO–CO–COH on reaction Site 17 from **Group 3** and the relevant adsorption energies (eV). Colour codes: Cu, orange; C, brown; O, red and H, pink. Red and blue values denote strong and weak *CO adsorption energies, respectively.

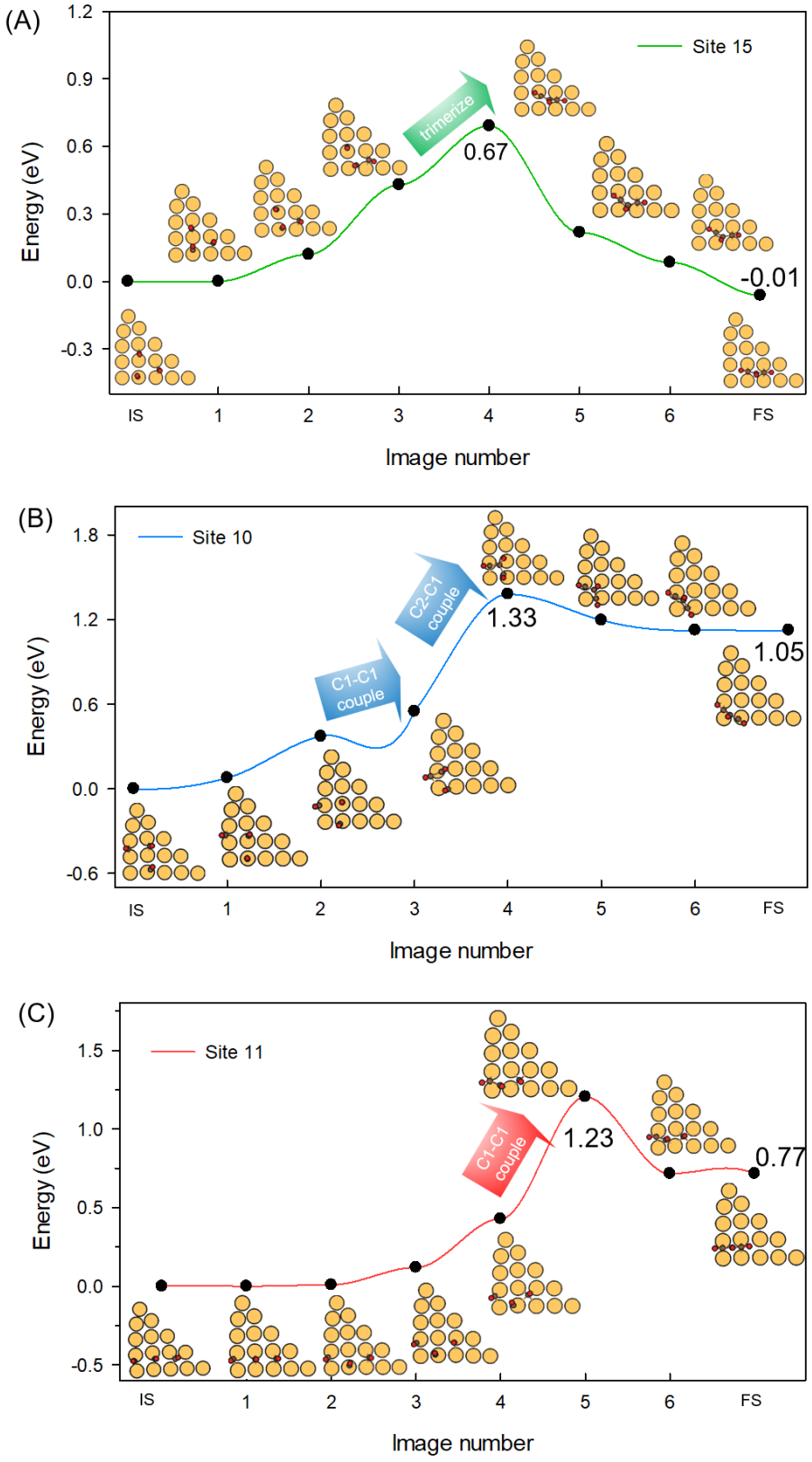

Figure S19. MEP involved in reaction *CO + *CO + *CO → *CO–CO–CO at 0 V vs RHE on reaction site (A) 15, (B) 10 and (C) 11. The reference energy level is set to be adsorption of 3*CO at 0 V vs RHE. The unit of energy is eV. Insets are atomistic structures of the initial, transition and final states. Colour codes: Cu, orange; C, brown; O, red.

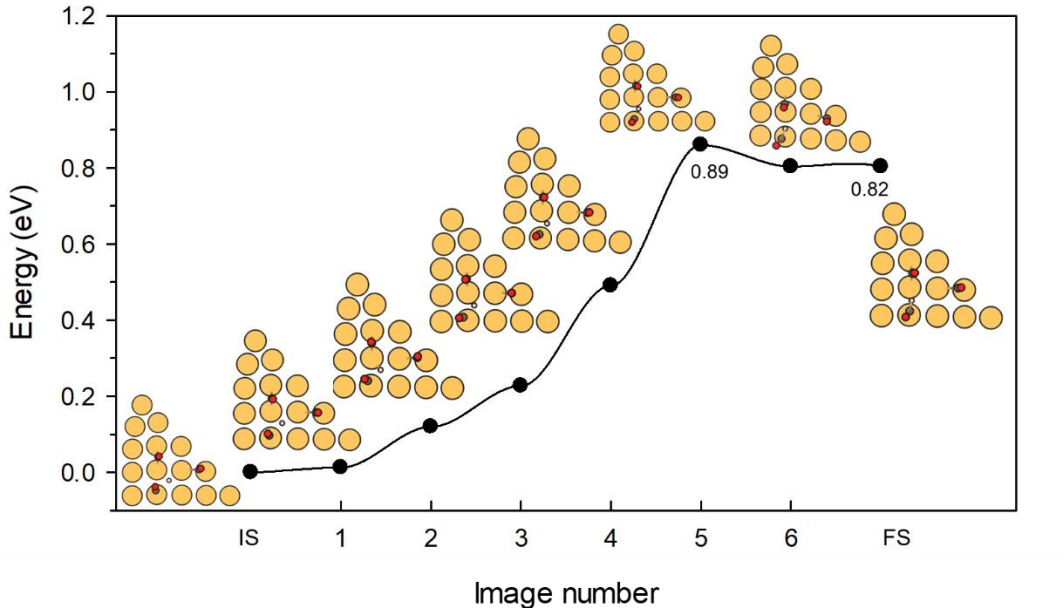

Figure S20. MEP involved in reaction 3*CO + *H → *CHO + 2*CO at 0 V vs RHE on reaction site 15. The reference energy level is set to be adsorption of 3*CO and *H at 0 V vs RHE. The unit of energy is eV. Insets are atomistic structures of the initial, transition and final states. Colour codes: Cu, orange; C, brown; O, red and H, pink.

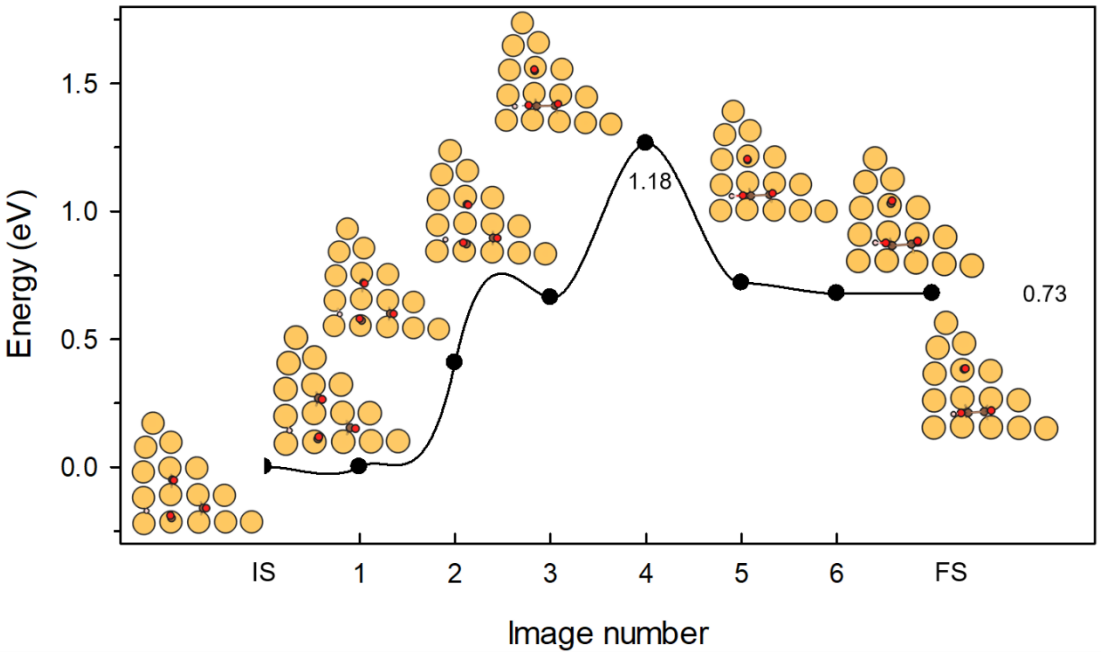

Figure S21. MEP involved in reaction 3*CO + *H → *CO–COH + *CO at 0 V vs RHE on reaction site 15. The reference energy level is set to be adsorption of 3*CO and *H at 0 V vs RHE. The unit of energy is eV. Insets are atomistic structures of the initial, transition and final states. Colour codes: Cu, orange; C, brown; O, red and H, pink.

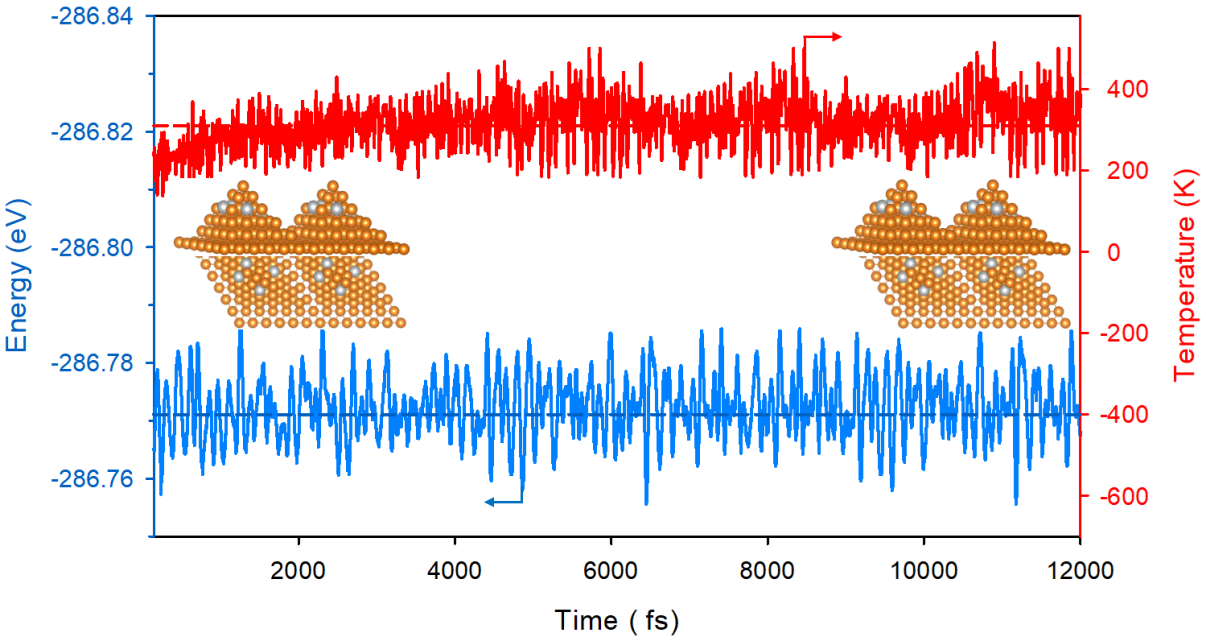

Figure. S22. Ab initio molecular dynamics (AIMD) simulated energy evolution for Ag/Cu-DAN at 300 K. Insets show the top and side views of the snapshots of atomic configurations at 0 and 12 ps. The blue and red dashed-lines denote equilibrium energy and temperature, respectively.

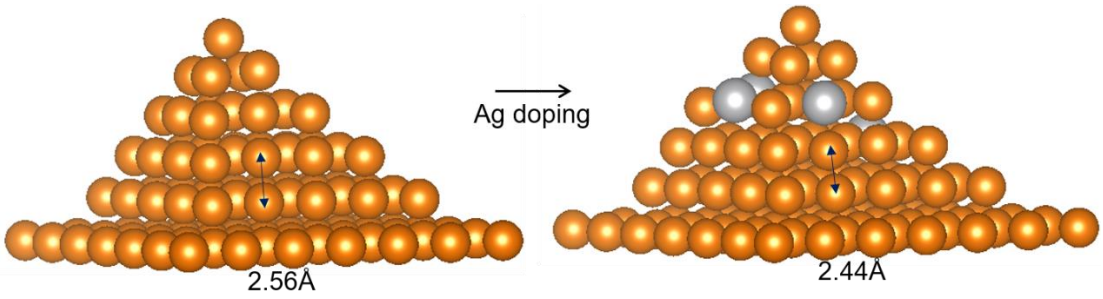

Figure S23. Upon Ag doping, the adjacent Cu–Cu bond length is decreased from 2.56 Å to 2.44 Å.

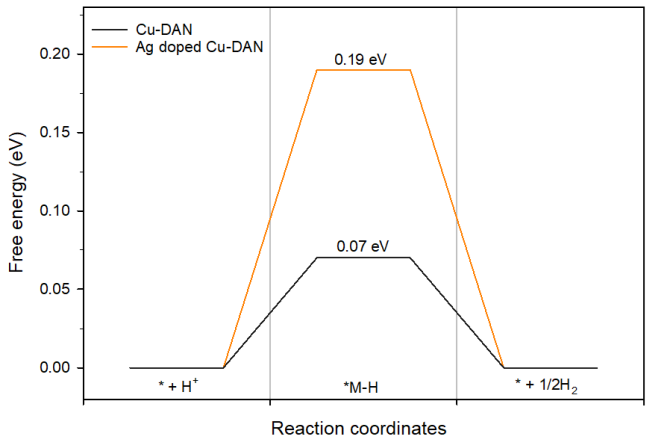

Figure S24. The free energy diagram of hydrogen evolution reaction on the Cu-DAN and Ag doped Cu-DAN.

Supplementary Note 1

Stability of Ag/Cu-DAN

Stability is a prerequisite for electrocatalytic materials. This is closely related to the experimental feasibility and catalytic activity for long-term use. we performed additional computational work to investigate (1) Cu/Ag dissolution possibility by dissolution potential (U_{diss}) analysis, and (2) thermodynamic stability by AIMD. Our calculation shows that under reaction potential, both Cu and Ag dissolution to the electrolyte is highly unlikely. U_{diss} is calculated as:[4]

$$U_{diss} = U^0_{diss(TM)} - E_f / ne$$

where $U^0_{diss(TM)}$ and n denote the standard reduction potential of transaction metal (TM) and the number of electrons transferred. E_f, the formation energy of one surface TM, is defined as

$$E_f = E_{nanopyramid} - E_{less} - E_{TM}$$

where $E_{nanopyramid}$ is the total energy, E_{less} is the energy of nanopyramid without one surface atom and E_{TM} is the energy of isolated TM.

The U^0_{diss} for Cu and Ag are 0.34 V (n=2) and 0.80 V (n=1), respectively. The calculated positive U_{diss} for Cu (1.72V) and Ag (2.14V) indicate that both atoms are stable under electrochemical environments.

In addition, we carried out further ab initio molecular dynamics (AIMD) simulations to explore the thermodynamic stability of the surface atoms of the Ag/Cu-DAN. The simulations were performed in NVT ensemble using Nose-Hoover thermostat at 300 K for 12 ps with a time step of 1 fs, as shown in Figure S22. We found that the thermal oscillations of surface Cu atoms occur near the equilibrium position, and the structure shows no severe structural distortion, suggesting that Cu-DAN can tolerate the thermal condition under CO_2RR.

Reference:

[1] L. Chen, C. Tang, Y. Jiao, S. Z. Qiao, *ChemSusChem*. 2020, **14**, 671-678.

[2] K. Jiang, Y. Huang, G. Zeng, F. M. Toma, W. A. Goddard, A. T. Bell, *ACS Energy Lett.*, 2020, **5**, 1206-1214.

[3] H. Shen, Y. Li and Q. Sun, *J. Phys. Chem. C*, 2017, **121**, 3963–3969.

[4] Y. Ouyang, L. Shi, X. Bai, Q. Li, J. Wang, *Chem*, *Sci.* 2020, **11**, 1807-1813.